

CENTRE FOR INSTRUCTOR AND ADVANCED SKILL TRAINING (CIAST)
DEPARTMENT OF SKILLS DEVELOPMENT
MINISTRY OF HUMAN RESOURCES

SkillsMalaysia Journal

Mechanical Properties of Dissimilar Aluminium Joints Using Friction Stir Welding (FSW)

Mohamad Riza Ismail¹, Zulkiflle Leman², Mohd Idris Shah Ismail³

¹Centre for Instructor and Advanced Skill Training (CIAST), Shah Alam, Selangor
^{2,3}Universiti Putra Malaysia, Serdang, Selangor

Abstract

This paper reviews on mechanical properties of dissimilar aluminium joints using friction stir welding (FSW). Friction stir welding (FSW) is becoming the choice of industry for structurally demanding applications. The applications of FSW are in marine, aerospace, railways, automotive, electrical and refrigerating industries. This process does not cause severe distortion and residual stresses as compared to traditional welding process. In this project, experiments were done to investigate the mechanical properties of AA1100-H14 (retreating side) and AA5052-H32 (advancing side) joints using FSW under combinations of three tool rotation speeds (1640, 1860 and 2050 rpm), two welding travel speeds (1.0 and 1.5 mm/s) and other specific parameters. Welding joints were went through two mechanical test; tensile test and microhardness test to obtain important properties such as ultimate tensile strength, yield strength, elongation and microhardness. Based on results, all joints showed good visual appearances but there was existence of wormhole along welding direction in several joints. In term of tensile strength, most of the joints produced high ultimate tensile strength and yield strength with more than 65% compare to AA1100-H14 properties. Meanwhile, there were significant dropped of hardness value in region 1 to 2.5 mm from weld centre in advancing side material due to the existence of wormhole. As conclusion, according to experiments result, combination of 2050 rpm (tool rotation speed) and 1.0 mm/s (welding travel speed) was the best combination that produced good external appearance, free from distortion and wormhole, relatively high ultimate tensile strength and yield strength values and also high microhardness value.

Keywords: Friction stir welding (FSW), mechanical properties, AA1100-H14, AA5052-H32, tool rotation speed, welding travel speed

Introduction

Friction stir welding (FSW) is a new innovation in welding technology. It was invented in 1991 [1] and become as major joining process for aluminium alloys, magnesium [2], titanium [13] and steel [4, 5]. It is extensively used in the aircraft industry and potentially a replacement for mechanical fastening. This technique is attractive for joining high strength aluminium alloys since there is far lower heat input during the process compare with conventional welding methods such as TIG or MIG [6]. In FSW, a non-consumable rotating tool with a specially designed pin and shoulders is inserted into abutting edges of sheets or plates to be joined and traversed along the line of joint [7].

In general, FSW has been used to weld all wrought aluminium alloys, across the 2xxx, 5xxx, 6xxx, and 7xxx series of alloys, some of which are bordering on being classed as virtually unweldable by fusion welding technique [8]. Considering the excellent capacity of friction stir welding in joining aluminium alloy with fewer metallurgical defects and less distortion compare to fusion welding, this new solid state welding will be highlighted to fabricate joints in similar and dissimilar aluminium alloys [9]. In addition, in

FSW the surface oxide is not deterrent for the process; no particular cleaning operations are needed prior to welding [10]. FSW does not produce sparks or flames. Thus, safety, environmental and legislation issues are not major concern [11].

FSW process was based on rotating the non-consumables tool to generate heat in the workpiece. This rotating tool is manufactured from materials with superior high temperature properties to those of the materials to be joined [12]. The working principle of FSW was illustrated as shown in Figure 1.

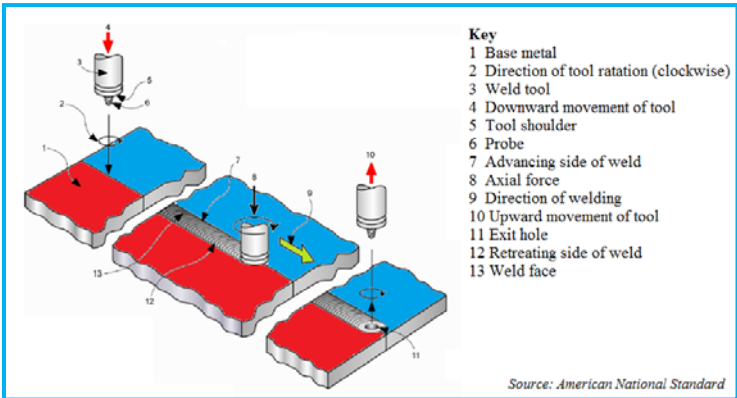


Figure 1: Working principle of friction stir welding [13]

Welding tools consist of shank, shoulder and pin is fixed in milling machine chuck and is rotated about its longitudinal axis [14]. The rotating tool then slowly plunged into the weld joint and forced to traverse along the joint line, heating the abutting components by interfacial and internal friction, thus producing a weld joint by extruding, forging and stirring the materials from the workpieces in the vicinity of the tool [15]. The half-plate where the direction of rotation is the same as that of welding is called the advancing side, with the other side designated as being the retreating side [16]. It is a crucial decision on locating which material in which side because both sides will experience different of conditions in term of heat transfer, material flow and other properties [17]. Figure 2 shows a clear view of advancing side and retreating side configuration.

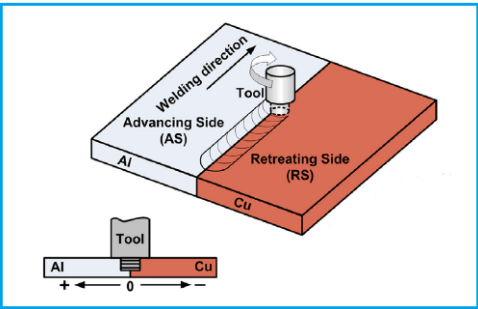


Figure 2: Advancing side and retreating side in FSW

The principal advantages of FSW summarized in Table 1;

Table 1: Advantages of FSW

Metallurgical Benefits	Environmental Benefits	Energy Benefits
<ul style="list-style-type: none"> • Solid-phase process • Low distortion of workpiece • Good dimensional stability • No loss of alloying elements • Fine microstructure • Absence of cracking 	<ul style="list-style-type: none"> • No shielding gas required • No surface cleaning required • Eliminate grinding wastes • Consumable materials saving, such as rags, wire or any other gases 	<ul style="list-style-type: none"> • Improved materials use • Decreased fuel consumption in light weight aircraft, automotive and ship applications

Selection of welding parameters, tool geometry and joint design will lead to different outcomes of weld. The setup of FSW will cause significant effect on the material flow pattern and temperature distribution and subsequently produced complex material movement and plastic deformation. It has been reported that tool rotation speed and welding travel speed have both direct and indirect influence to the final joint. Low tool rotation speed induces low stirring effect and finally low heat generation rate while low welding travel speed increases exposure to heat source, facilitate more material flow and reduced multi component loads. Table 2 briefly explained about main process parameters in FSW and its effects;

Table 2: Main parameter in FSW and its effects

Parameter	Effects
Rotating speed (rpm)	Frictional heat, stirring, oxide layer breaking and mixing of material
Tilting angle (°)	Appearance, thinning
Welding travel speed (mm/s)	Appearance, heat control
Down force (kN)	Frictional heat, maintaining contact conditions

It is important to get better understanding on the typical cross-section of FSW joints. During the FSW, the materials undergo plastic deformation due to elevated heating. The grain become finer and equiaxed recrystallized. Normally, cross-section of FSW joints will consist four zones namely base metal zone (BM), heat-affected zone (HAZ), thermo-mechanical affected zone (TMAZ) and stirred or nugget zone (SZ).

HAZ is zone where the maximum peak temperature is significantly lower than the solidus temperature and heat source is rather diffuse. SZ is the zone which experiences the most severe deformation and containing the onion ring appearance meanwhile TMAZ lies between HAZ and SZ. Figure 3 shows the cross section of FSW joints.

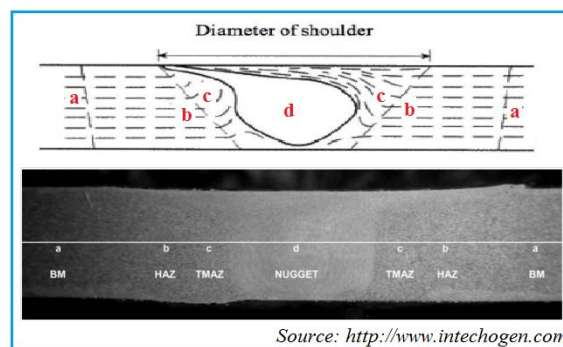


Figure 3: Cross section of FSW joints

Tool design influences heat generation, plastic flow, the power required and the uniformity of the welded joint. The shoulder generates most of the heat and prevents the plasticized material from escaping from the workpiece, while both the shoulder and the pin tool affect the material flow. FSW can be performed with tool of a simple geometry yet having good mechanical properties. Advanced tool design provides intensified material flow in the stirred zone and better weld quality.

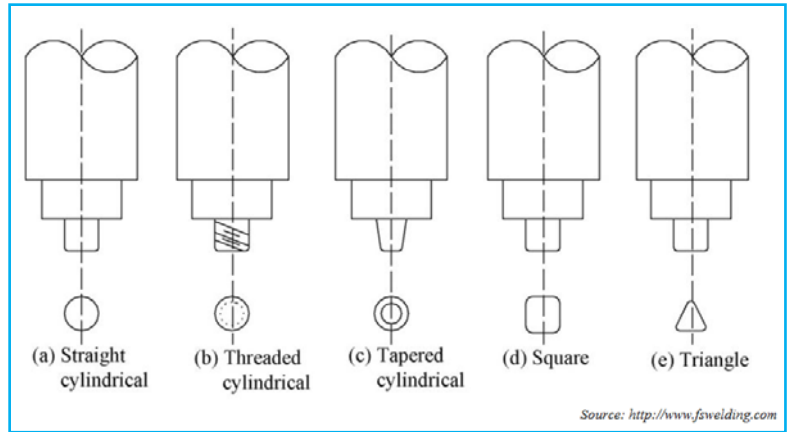



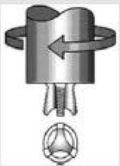




Figure 4: Basic FSW tool pin profiles

Tool	Cylindrical	Whorl™	MX triflute™	Flared triflute™	A-skew™	Re-stir™
Schematics						
Tool pin shape	Cylindrical with threads	Tapered with threads	Threaded, tapered with three flutes	Tri-flute with flute ends flared out	Inclined cylindrical with threads	Tapered with threads

Source: http://www.fswelding.com

Figure 5: Advanced FSW tools developed at The Welding Institute, Cambridge

Experimental Procedures

For this project, straight cylindrical tool design had been used. Tool was fabricated from low carbon steel round bar with 15 mm in diameter and 125 mm length using conventional turning machine (ZMM-Sliven C8C) to intended size as illustrated in Figure 6. This material has been selected because it had significantly higher strength and hardness than aluminium AA1100-H14 and AA5052-H32.

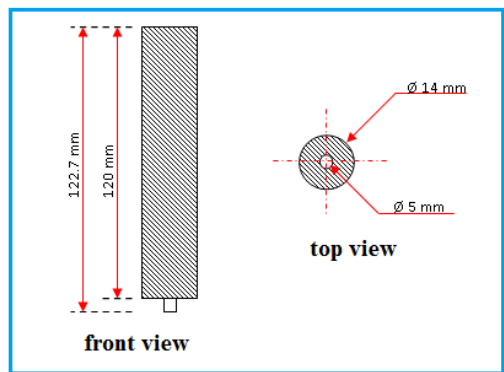


Figure 6: Tool design

This experiment used two series of aluminium; AA1100-H14 and AA5052-H32. Materials in sheet plate was cut using jigsaw to required size. Dimensions of the workpieces were 100 mm length x 50 mm width x 3 mm thickness. Table 3 and 4 shows the

chemical compositions and mechanical properties for both materials respectively while figure 7 illustrated the dimensions of the materials.

Table 3: Chemical properties and mechanical properties of AA1100-H14 [18]

AA1100-H14			
Chemical Compositions			
Aluminum, Al	Copper, Cu	Manganese, Mn	Other, each
≥99.00%	0.05-0.20%	≤0.05%	≤0.05%
Silicon (Si) + Ferrum (Fe)	Zinc, Zn	Other, total	Beryllium, Be
≤0.95%	≤0.10%	≤0.15%	≤0.0008 %
Mechanical Properties			
Ultimate Tensile Strength (MPa)	Yield Strength (MPa)	Elongation at Break	Hardness (Brinell - AA; Typical; 500 g load; 10 mm ball)
124	95	1.0-10%	23

Source: <http://www.matweb.com>

Table 4: Chemical properties and mechanical properties of AA5202-H32 [19]

AA5202-H32				
Chemical Compositions				
Aluminum, Al	Copper, Cu	Chromium, Cr	Other, each	Silicon, Si
95.7-97.7 %	≤0.10 %	0.15-0.35%	≤0.05%	≤0.25%
Zinc, Zn	Other, total	Magnesium, Mg	Manganese, Mn	Iron, Fe
≤0.10%	≤0.15%	2.2-2.8 %	≤0.10%	≤0.40%
Mechanical Properties				
Ultimate Tensile Strength (MPa)	Yield Strength (MPa)	Elongation at Break	Hardness (Brinell - AA; Typical; 500 g load; 10 mm ball)	
228	193	12%	60	

Source: <http://www.matweb.com>

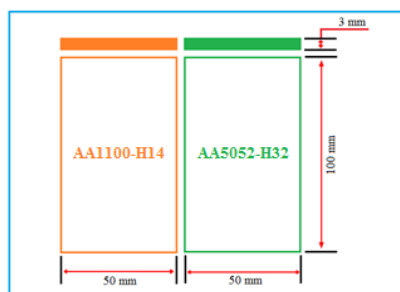


Figure 7: Dimensions of material

This FSW experiment was carried out using conventional vertical milling machine (Johnford Model 2VS) with some modifications (Figure 8). Milling table speed was control through motorised controller and spindle rotation speed was measured using digital photo/contact tachometer. Simple clamping fixture designed and fabricated from low carbon steel sheet plate 10 mm thickness to grip the materials as in Figure 9.



Figure 8: Vertical milling machine Johnford Model 2VS

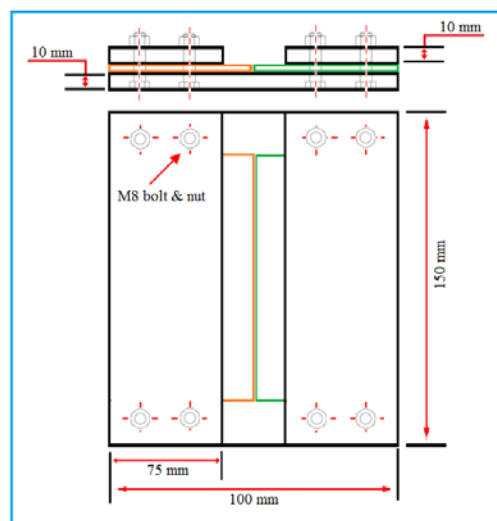


Figure 9: Clamping fixture design

In this experiment, AA1100-H14 had been selected as retreating side while AA5052-H32 as advancing side. FSW was done using six combinations of tools rotation speeds and travel speeds. These combinations were selected by referring to previous research done by previous researcher. Tool tilt angle was set to 0° . The pin length was set to 2.7 mm, means that it is 3 mm less than material thickness. Low carbon steel plate bar of 10 mm thickness was used as backing plate in this experiment.

Welding conditions for this experiment can be summarized as below;

Table 5: Welding condition for FSW experiment

Process Parameter	Value
Material location	AA1100-H14 (RS); AA5052-H32 (AS)
Tool rotation speed (rpm)	1640, 1860, 2050
Travel speed (mm/s)	1, 1.5
Tool tilt angle (°)	0
Tool shoulder diameter (mm)	14
Tool shoulder surface	flat
Pin diameter (mm)	5
Pin length (mm)	2.7
Backing plate	Yes

The welded materials then went through the tensile testing to measure the mechanical properties of the joint such as ultimate tensile strength, yield strength and the elongation. Using CNC milling machine, specimen was cut to required shape and dimensions according ASTM E8/E8M-11. Tensile test was run using Instron 3366 with maximum capacity of 10 kN.

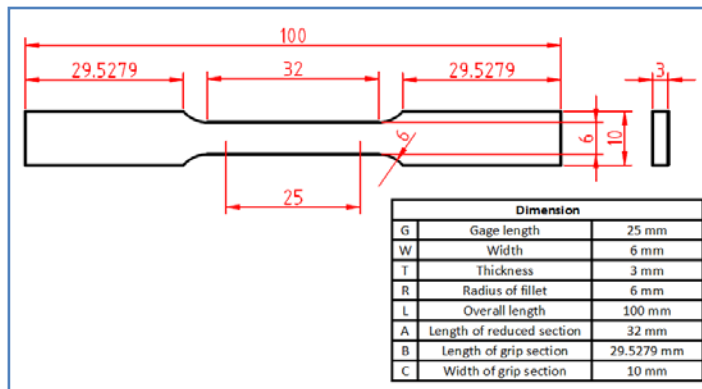


Figure 10: Dimensions of tensile testing specimen according to ASTM E8/E8M-11

Microhardness test was carried out to the welding specimens in order to study the weld structure of FSW. The measurement was made on a cross section and perpendicular to the welding direction. Before the test can be done, the specimens went through several processes such as mounting, curing, grinding and polishing in order to obtain clean and fine surface. Microhardness testing was done using Wolpert Group micro-Vickers hardness tester digital 401 MVD. The measurement was taken at 0.635 mm offset from weld centre.

Results and Discussions

Visual observation was discovered several findings. The top and bottom surface of the welding shows an excellent appearance. Both materials were seemed to mix very well. The joints were also free from distortion.

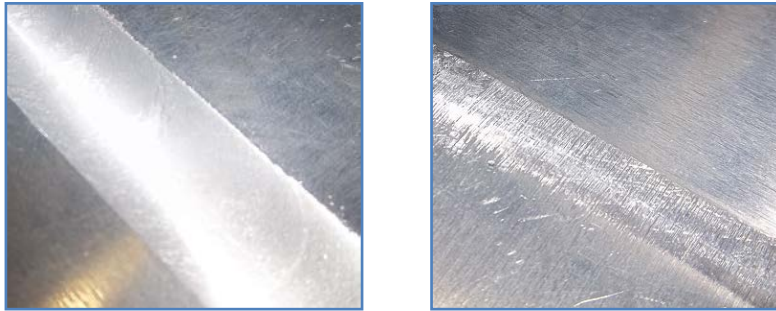


Figure 11: Top and bottom surface of the joint



Figure 12: Joint free from distortion

From the welding cross section, the existence of wormhole or tunnel defect was identified along welding direction. This hole was located in advancing side (AA5052-H32) and at the edge of pin diameter. Centre of hole was located within 1.7 to 1.9 mm from the top surface and the sizes were in range of 0.48 to 1.21 mm². Wormhole or channel defect were very serious deflection, which affects the tensile properties and elongation percentage greatly, and decreases the tensile strength and elongation percentage sharply [20]. At a constant rotational speed, an increase in the travel speed leads to wormhole initiation near the bottom of the weld [16]. Furthermore, the size of the wormholes increases with the travel speed because of inadequate material flow towards the bottom of the weld [21]. There are indications that the travel speed to rotational speed ratio is an important variable in the formation of the wormhole defect [22]. In brief, the defects may happen because of insufficient heat generation by tool shoulder and can be solve through optimizing the process parameters, particularly by reducing the welding travel speed and increasing the tool rotation speed.

Referred to graph (load vs. Extension) obtained from tensile testing report, values of yield load and yield extension for all combination can be measured. To simplify the comparison of ultimate tensile strength and yield strength between joint and base material, related graph was constructed according to data in Table 6.

Table 6: Ultimate tensile strength and yield strength values between parameters

Parameter	Yield strength (MPa)	Ultimate tensile strength (MPa)
1640 rpm; 1.0 mm/s	33.33	62.21
1860 rpm; 1.0 mm/s	48.89	79.69
2050 rpm; 1.0 mm/s	55.56	93.46
1640 rpm; 1.5 mm/s	61.11	102.32
1860 rpm; 1.5 mm/s	58.33	88.94
2050 rpm; 1.5 mm/s	55.56	97.53
AA1100-H14*	95	124
AA5052-H32*	193	228

* Source: <http://www.matweb.com>

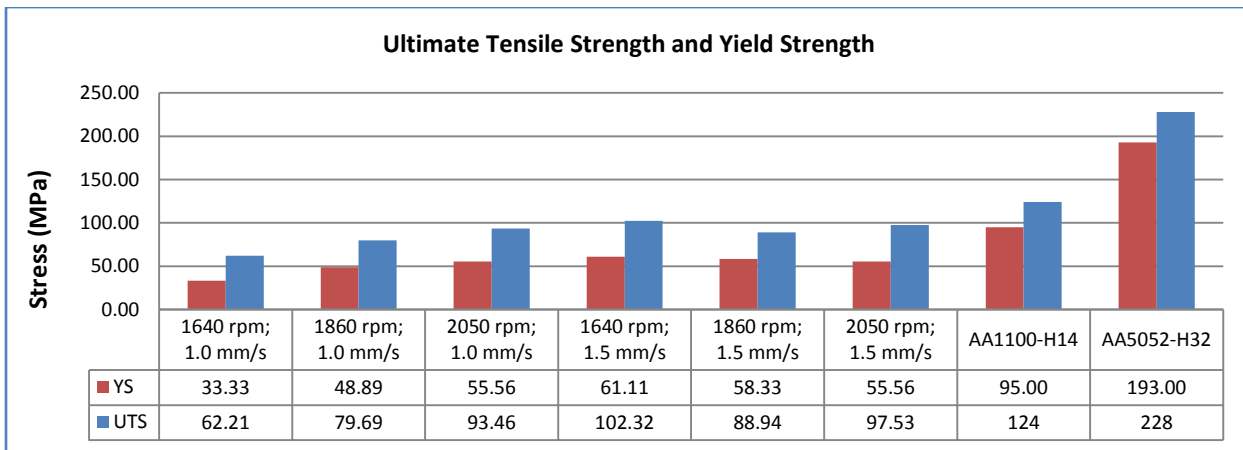


Figure 13: Graph of ultimate tensile strength and yield strength

Elongation at break for each parameter was as shown in Table 7.

Table 7: Elongation at break for each parameter and base material

Parameter	Maximum elongation (mm)	Gauge length (mm)	Elongation at break (%)
1640 rpm; 1.0 mm/s	0.90623	25.00	3.62492
1860 rpm; 1.0 mm/s	2.34564	25.00	9.38256
2050 rpm; 1.0 mm/s	4.51265	25.00	18.0506
1640 rpm; 1.5 mm/s	3.84162	25.00	15.3665
1860 rpm; 1.5 mm/s	1.20596	25.00	4.82384
2050 rpm; 1.5 mm/s	2.06660	25.00	8.2664
AA1100-H14*			10
AA5052-H32*			12

* Source: <http://www.matweb.com>

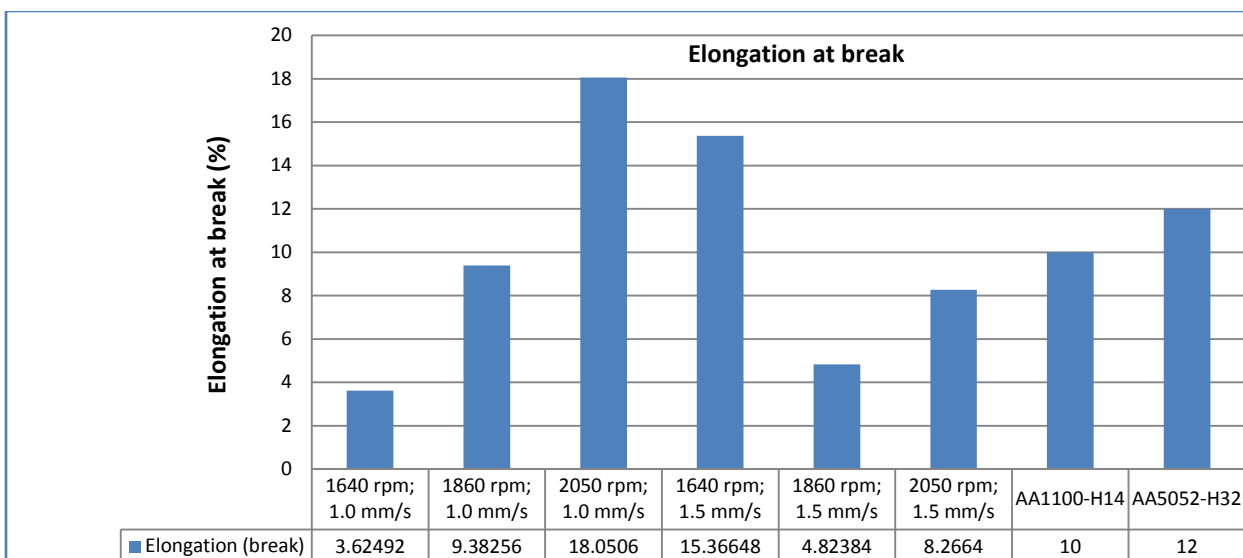


Figure 14: Elongation at break among parameter and base material

Stress-strain curve was constructed as depicted in Figure 15.

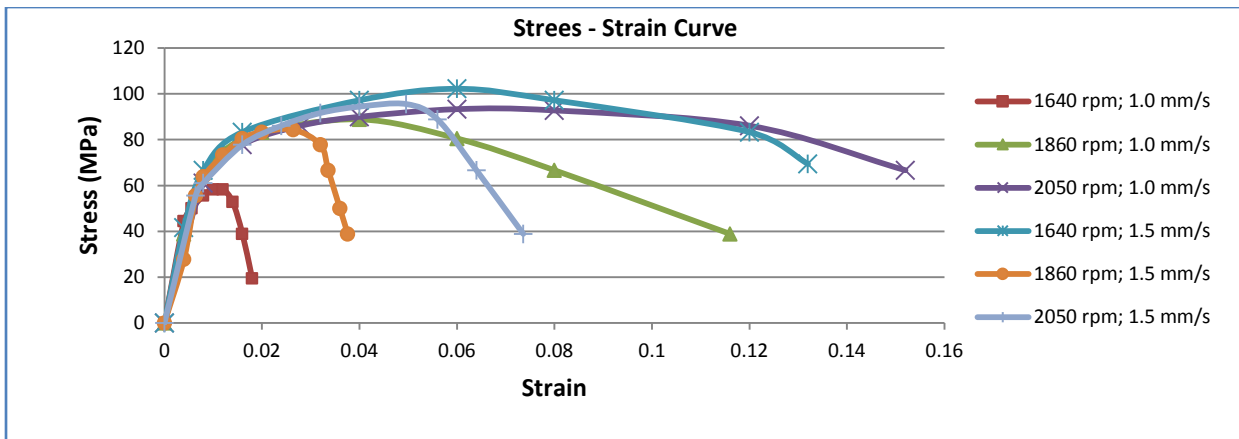


Figure 15: Stress-strain curve among parameters

Investigating the ultimate tensile strength and yield strength and compare it with base material properties shows that this type of process have a good potential to be improve to produce better result. The minimum values of ultimate tensile strength and yield strength were obtained from parameter 1640 rpm & 1.0 mm/s with value of 62.21 MPa and 33.33 respectively. These values were less than 50% of AA1100-H14. Meanwhile, maximum values of ultimate tensile strength and yield strength were obtained from parameter 1640 rpm; 1.5 mm/s with value of 102.32 MPa and 61.11 respectively. Four of the parameters produced high ultimate tensile strength and yield strength with more than 65% compare to AA1100-H14 properties.

The elongation of specimen represented that some parameter produced a good ductility. Parameter 2050 rpm & 1.0 mm/s and 1640 rpm & 1.5 mm/s produced joints with elongation percentage higher than base material.

Microhardness test was done on mid-thickness of the joint using Vickers method. The measurement was 0.635 mm offset starting from weld centre. The result for the test was as illustrated in Table 8 and Figure 16.

Table 8: Result of microhardness testing on FSW specimens

Base material	Distance from weld centre (mm)	Parameter					
		1640 rpm; 1.0 mm/s	1860 rpm; 1.0 mm/s	2050 rpm; 1.0 mm/s	1640 rpm; 1.5 mm/s	1860 rpm; 1.5 mm/s	2050 rpm; 1.5 mm/s
AA1100-H14	-3.81	29.4	28	28.2	29.6	28.2	29.4
	-3.175	29.8	28.1	32.3	29	27.3	29.3
	-2.54	29.4	28.5	27.9	28.2	28.8	29.4
	-1.905	23.9	28.9	28.6	29.9	28.3	29.2
	-1.27	60.9	47.2	58.3	61	58.7	58.3
	-0.635	60.8	56.5	53.6	58	58.3	58.1
center	0	56.4	56.5	52.2	56.9	49.7	57.7
AA5052-H32	0.635	36	57.2	54.8	56.7	35	53.4
	1.27	19.9	19.9	54	30.2	18	18
	1.905	27.7	24.9	54.1	53.8	54.5	55.8
	2.54	54	55.8	54.3	53.6	53.8	54.2
	3.175	55	53.6	53.6	52.9	54.2	55.1
	3.81	53.8	53.7	53.7	53.6	53.6	52.8

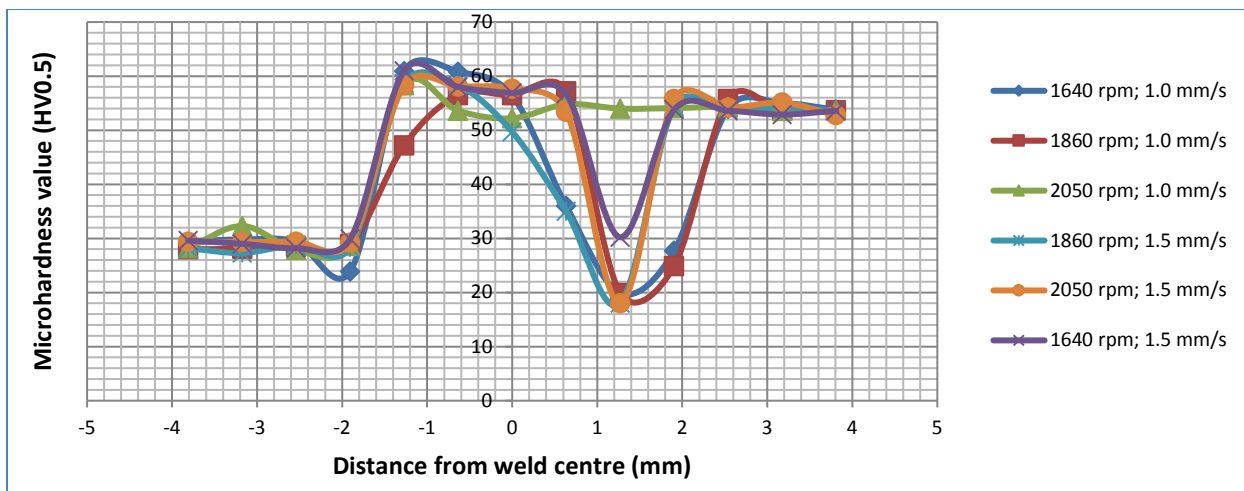


Figure 16: Microhardness properties of the experiment

From microhardness data and graph, it shows that the material was flow from advancing side to retreating side. This can be proved by referring to increasing values of hardness in retreating side. It is mean that, material from AA5052-H32 that was harder than AA1100-H14 was flow across the material boundary and mixed with AA1100-H14.

There was significant dropped of hardness value in region 1 mm to 2.5 mm from weld centre in advancing side material. This can be explained by the existence of wormhole along the welding direction. However, parameter 2050 rpm & 1.0 mm/s produced excellent result of microhardness because there was no defect in the joint.

Conclusion

The objectives of the research to characterize the mechanical properties through tensile test and microhardness test of friction stir welding on dissimilar aluminium AA1100-H14 and AA5052-H32 was successfully achieved. Data and graph generate from the testing provided useful information on determining the optimal conditions of FSW to obtaining the best welded joint.

Parameter 2050 rpm of tool rotation speed and 1.0 mm of welding travel speed was selected as the best combination since it provide high ultimate tensile strength and yield strength, good in elongation and free from defect either on surface on inside the joint. Furthermore, this combination produced excellent result of microhardness.

References

- [1] W.M. Thomas, E.D. Nicholas, J.C. Needham, M.G. Murch, P. Temple-Smith and C.J. Dawes. (1991). Friction Stir Butt Welding, International Patent No. PCT/GB92/02203
- [2] T. Nagasawa, M. Otsuka, T. Yokota and T. Ueki. (2000). Magnesium Technology, Minerals and Metal Society, pp. 383-387
- [3] M.C. Juhas, G.B. Viswanathan and H.L. Fraser. (2000). 2nd International Symposium on FSW, TWI
- [4] A.P. Reynolds, W. Tang, T. Gnaupel-Herold and H. Prask. (2003). Scripta Mater, vol 48 (9), pp. 1289-1294
- [5] W.M. Thomas, P.L. Threadgill and E.D. Nicholas. (1999). Science Technology Welding Joining, vol. 4 (6), pp. 365
- [6] H.S. Patil and S.N. Soman. (2010). Experimental Study on the Effect of Welding speed and Tool Pin Profiles on AA6082-O Aluminium Friction Stir Welded Butt Joints, International Journal of Engineering, Science and technology
- [7] Sivaprakasam Thamizhmanii, Mohd Azizie Shukor and Sulaiman. (2013). Solid State Friction Stir Welding (FSW) on Similar and Dissimilar Metals, Preceeding of the World Congress on Engineering 2013 vol III
- [8] Vijay Soundarajan, Eswar Yarrapareddy and Radovan Kovacevic. (2007). Investigation of the Friction Stir lap Welding of Aluminium Alloys AA5182 and AA6022, Journal of materials Engineering and Performance Vol. 16(4)
- [9] Youbao Song, Xinqi Yang, Lei Cui, Xiaopeng Hou, Zhikang Shen and Yan Xu. (2014). Defect Features and Mechanical Properties of Friction Stir lap Welded Dissimilar AA2024-AA7075 Aluminium Alloy Sheets, Material and Design 55
- [10] P. Cavaliere, E. Cerri and A. Squillace. (2005). Mechanical Response of 2024-7075 Aluminium Alloys Joined by Friction Stir Welding, Journal of Materials Science 40, pp. 3669-3676
- [11] Khairuddin et al. (2012). Principles and Thermo-Mechanical Model of Friction Stir Welding, InTech

- [12] Wayne M. Thomas, Keith I. Johnson and Christoph S. Wiesner. (2003). Friction Stir Welding – Recent Developments in Tool and Process technologies, *Advanced Engineering Material*
- [13] AWS. (n.d). Draft 16 – AWS D17.3/D17.3M:200X Specification for Friction Stir Welding of Aluminum Alloys for Aerospace Hardware, American National Standard, American Welding Society.
- [14] Mandeep Singh Sidhu and Sukhpal Singh Chatha. (2012). Friction Stir Welding – Process and Its Variables: A Review, *International Journal of Emerging Technology and Advanced Engineering*
- [15] Pedro Vilaca and Telmo G. Santos. (2011). Non-Destructive testing Techniques for Detecting Imperfections in Friction Stir Welding of Aluminium Alloys, *Aluminium Alloy, Theory and Applications*, ISBN: 978-953-307-244-9, InTech
- [16] R. Nandan, T. DebRoy and H. K. D. H. Bhadeshia. (2008). Recent Advances in Friction Stir Welding – Process, Weldment Structure and Properties, *Progress in Materials Science* 53
- [17] Jae-Hyung Cho, Donald E. Boyce and Paul R. Dawson. (2005). Modeling Strain Hardening and Texture Evolution in Friction Stir Welding of Stainless Steel, *Materials Science and Engineering A* 398
- [18] MATWEB. (2014). Material Property Data: Aluminum AA1100-H14. Retrieved from <http://www.matweb.com/search/DataSheet.aspx?MatGUID=c0652f2efeac49b89b50e7e4c6fba759>
- [19] MATWEB. (2014). Material Property Data: Aluminum AA5052-H32. Retrieved from <http://www.matweb.com/search/DataSheet.aspx?MatGUID=96d768abc51e4157a1b8f95856c49028>
- [20] Hua-Bin Chen, Keng Yan, Tao Lin, Shan-Ben Chen, Cheng-Yu Jiang and Yong Zhao. (2006). The Investigation of Typical Welding Defects for 5456 Aluminum Alloy Friction Stir Welds, *Materials Science and Engineering, A* 433 64 – 69
- [21] R. Crowford, G. E. Cook, A. M. Strauss, D. A. Hartman and M. A. Stremmler. (2006). Experimental defect analysis and force prediction simulation of high weld pitch friction stir welding, *Science and Technology of Welding and Joining*, 11: 657 – 665
- [22] H. J. Liu, H. Fujii, M. Maeda and K. Nogi. (2004). Tensile Fracture location characterisation of Friction Stir Welded Joints of Different Aluminium Alloys, *Journal of Materials Science and Technology*, 20: 103 – 105